

Correspondence

Gold Nanolenses Generated by Laser Ablation-Efficient Enhancing Structure for Surface Enhanced Raman Scattering Analytics and Sensing

Janina Kneipp,^{*,†,‡} Xiangting Li,[§] Margaret Sherwood,[†] Ulrich Panne,[‡] Harald Kneipp,[†] Mark I. Stockman,[§] and Katrin Kneipp^{†,||}

Wellman Center for Photomedicine, Harvard University Medical School, Boston, Massachusetts 02115, Federal Institute for Materials Research and Testing, Berlin, Germany, Department of Physics and Astronomy, Georgia State University, Atlanta, Georgia 30302, and Harvard-MIT Division of Health Sciences and Technology, Cambridge, Massachusetts 02139

Nanoaggregates formed by metal spheres of different radii and interparticle distances represent finite, deterministic, self-similar systems that efficiently concentrate optical fields and act as “nanolenses”. Here we verify experimentally the theoretical concept of nanolenses and explore their potential as enhancing nanostructures in surface enhanced Raman scattering (SERS). Self-similar structures formed by gold nanospheres of different sizes are generated by laser ablation from solid gold into water. These nanolenses exhibit SERS enhancement factors on the order of 10^9 . The “chemically clean” preparation process provides several advantages over chemically prepared nanoaggregates and makes the stable and biocompatible gold nanolenses potent enhancing structures for various analytical and sensing applications.

Surface enhanced Raman scattering (SERS) is one of the most impressive applications of enhanced local optical fields near metallic nanostructures due to their plasmon resonances.^{1,2} Aggregates formed by gold and silver nanoparticles are very popular enhancing structures in SERS with applications reaching from single molecule Raman spectroscopy^{3–5} to ultrasensitive probing in live cells.^{6–8}

In most cases, gold and silver nanoparticles are made in a chemical reduction process⁹ or by radiolytic techniques.^{10,11} Small aggregates are the outcome of the chemical preparation process or are formed by the addition of an aggregation-inducing agent to the colloidal solution, such as various salts. The chemical preparation of metal nanostructures can result in impurities on the surface of the metal, mainly due to residual anions and the reducing agent, which can give rise to surface enhanced Raman signals.¹² At low concentrations of the analyte, SERS signals of these impurities appear at the same level as the signals originating from the analyte and the SERS spectrum of the target molecule can vanish in the nonspecific background of the impurities.¹³

Generating metal nanoparticles in solutions by laser ablation is a promising alternative to chemical preparation.^{14–18} Laser irradiation does not only ablate nanoparticles from bulk metals. When interacting with metal nanoparticles, it can also change the morphology of these nanoparticles.^{19,20} Different mechanisms can be responsible for the ablation process: In addition to explosive boiling, there are also nonthermal pathways that are operative at short laser pulses.²¹ Recently, ablation was demonstrated with

(8) Kneipp, J.; Kneipp, H.; Wittig, B.; Kneipp, K. *Nano Lett.* **2007**, *7*, 2819–2823.

(9) Lee, P. C.; Meisel, D. *J. Phys. Chem.* **1982**, *86*, 3391–3395.

(10) Henglein, A. *J. Phys. Chem.* **1993**, *97*, 5457–5471.

(11) Henglein, A.; Meisel, D. *Langmuir* **1998**, *14*, 7392–7396.

(12) Munro, C. H.; Smith, W. E.; Garner, M.; Clarkson, J.; White, P. C. *Langmuir* **1995**, *11*, 3712–3720.

(13) Kneipp, K. *Exp. Tech. Phys.* **1988**, *36*, 161–166.

(14) Fojtik, A.; Henglein, A. *Ber. Bunsen-Ges. Phys. Chem.* **1993**, *97*, 252.

(15) Nedderson, J.; Chumanov, G.; Cotton, T. *Appl. Spectrosc.* **1993**, *47*, 1959.

(16) Brause, R.; Moltgen, H.; Kleinermanns, K. *Appl. Phys. B* **2002**, *75*, 711–716.

(17) Tsuji, T.; Iryo, K.; Nishimura, Y.; Tsuji, M. *J. Photochem. Photobiol., A* **2001**, *145*, 201–207.

(18) Sylvestre, J. P.; Poulin, S.; Kabashin, A. V.; Sacher, E.; Meunier, M.; Luong, J. H. T. *J. Phys. Chem. B* **2004**, *108*, 16864–16869.

(19) Besner, S.; Kabashin, A. V.; Meunier, M. *Appl. Phys. A* **2007**, *88*, 269–272.

(20) Tsuji, T.; Okazaki, Y.; Higuchi, T.; Tsuji, M. *J. Photochem. Photobiol., A* **2006**, *183*, 297–303.

(21) Stuart, B. C.; Feit, M. D.; Herman, S.; Rubenchik, A. M.; Shore, B. W.; Perry, M. D. *J. Opt. Soc. Am. B: Opt. Phys.* **1996**, *13*, 459–468.

* To whom correspondence should be addressed. E-mail: kneipp@usa.net.

† Harvard University Medical School.

‡ Federal Institute for Materials Research and Testing.

§ Georgia State University.

|| Harvard-MIT Division of Health Sciences and Technology.

(1) Willets, K. A.; Van Duyne, R. P. *Annu. Rev. Phys. Chem.* **2007**, *58*, 267–297.

(2) Lal, S.; Link, S.; Halas, N. J. *Nat. Photonics* **2007**, *1*, 641–648.

(3) Kneipp, K.; Yang, W.; Kneipp, H.; Perelman, L. T.; Itzkan, I.; Dasari, R. R.; Feld, M. S. *Phys. Rev. Lett.* **1997**, *78*, 1667–1670.

(4) Xu, H. X.; Bjerneld, E. J.; Kall, M.; Borjesson, L. *Phys. Rev. Lett.* **1999**, *83*, 4357–4360.

(5) Michaels, A. M.; Nirmal, M.; Brus, L. E. *J. Am. Chem. Soc.* **1999**, *121*, 9932–9939.

(6) Kneipp, J.; Kneipp, H.; McLaughlin, M.; Brown, D.; Kneipp, K. *Nano Lett.* **2006**, *6*, 2225–2231.

(7) Kneipp, K.; Kneipp, H.; Kneipp, J. *Acc. Chem. Res.* **2006**, *39*, 443–450.

femtosecond pulses at low pulse energies, exploiting the optical near-field of the metal nanoparticles themselves also for the ablation process.²²

Silver and gold nanoparticles made by laser ablation have been also used in several SERS applications,^{15,23–25} but so far, these ablated structures exhibited only modest SERS enhancement factors, always much lower than those obtained for chemically prepared nanoaggregates.

Here we show that ablation processes can produce stable gold nanoaggregates that provide a very high enhancement level. We discuss this finding in terms of a strong electromagnetic SERS enhancement for self-similar metal structures, verify experimentally the theoretical concept of nanolenses,^{26–28} and demonstrate the potential of these aggregates as enhancing nanostructures in SERS.

EXPERIMENTAL SECTION

Ablation of Gold Nanoparticles. For the preparation of gold nanoparticles, 1064 nm laser pulses with pulse lengths of 10 ns, a repetition rate of 10 Hz, and pulse energies of ~ 0.3 Ws were focused in a spot of ~ 0.5 mm onto gold foil in deionized water. Ablation was performed in 20 mL water over 50 min. The concentration of uniform gold nanospheres (see for example structures A in Figure 1) can be inferred from the absorbance to be on the order of 10^{-9} M.²⁹

Uniform gold spheres were only generated in ablation experiments, in which the laser penetrated only a thin layer (1–2 mm) of water on top of the gold foil. For thicker layers of water, the ablation process resulted in gold spheres of varying sizes between 100 and 7 nm with a tendency to form nanoaggregates. The differences between these two types of ablation processes might be explained by the fact that in the latter case of the heterogeneous nanoaggregates, the laser does not only ablate nanospheres from the bulk gold. On its way through the solution of gold nanoparticles, it also changes the morphology of the suspended particles. The mechanism of these complex processes during interaction of laser pulses and metal nanoparticles is a field of active research.^{19,21,22}

Chemical Preparation of Gold Nanoparticles. Gold nanoparticles in a size range between 30 and 50 nm were produced by chemical preparation as described in ref 9, resulting in colloidal solutions comprised by isolated nanoparticles and small aggregates (see for example structures B in Figure 1).

Because of this size variation, the particle concentration can only be roughly estimated from the absorbance of the gold sol to be on the order of 10^{-10} M. This value is in good agreement with

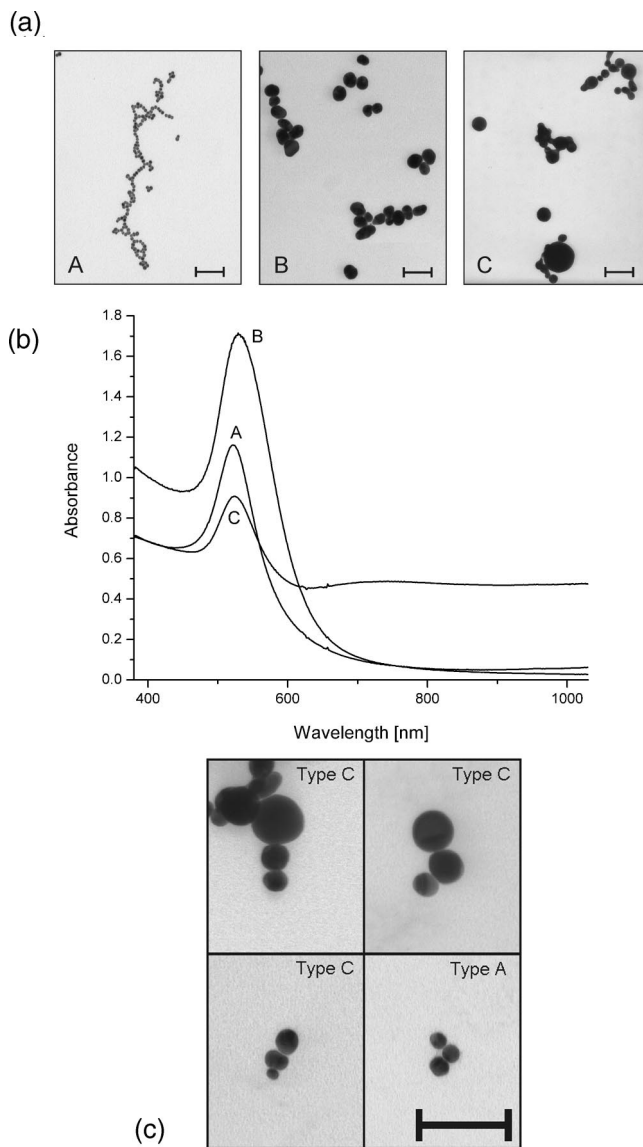


Figure 1. Electron micrographs of gold nanostructures and extinction spectra of their aqueous solutions: (a) Image A shows small uniform spheres generated by ablating gold from the bulk material. For comparison, image B displays gold nanoparticles made in a chemical reduction process. Image C shows nanoaggregates consisting of spheres with significantly different radii. These so-called “nanolenses” are generated due to ablation *and* interaction of the laser with the suspended ablated gold spheres. Scale bars: 100 nm. (b) Extinction spectra of the aqueous solutions of the nanostructures of types A, B, and C, respectively, corresponding to the micrographs shown in parts a and c. (c) Examples of small ablation aggregates composed from gold spheres of about same sizes (type A) and nanolenses (type C). Scale bar: 100 nm.

the total amount of gold available in the sol for the chemical process.

Raman Measurements. Raman measurements were performed at 785 nm excitation using a single monochromator equipped with edge filters and a CCD detector. SERS spectra were acquired in 20 μ L drops of nanoparticle solutions with adenine added. A 60 \times water immersion objective was used for directing the excitation laser onto the sample and for collection of the Raman scattered light.

- (22) Plech, A.; Kotaidis, V.; Lorenc, M.; Boneberg, J. *Nat. Phys.* **2006**, *2*, 44–47.
 (23) Prochazka, M.; Stepanek, J.; Vlckova, B.; Srnova, I.; Maly, P. *J. Mol. Struct.* **1997**, 410–411; 213–216.
 (24) Kneipp, K.; Kneipp, H.; Kartha, V. B.; Manoharan, R.; Deinum, G.; Itzkan, I.; Dasari, R. R.; Feld, M. S. *Phys. Rev. E* **1998**, *57*, R6281–R6284.
 (25) Ding, L. P.; Fang, Y. *Appl. Surf. Sci.* **2007**, *253*, 4450–4455.
 (26) Li, K. R.; Stockman, M. I.; Bergman, D. J. *Phys. Rev. Lett.* **2003**, *91*, 227402.
 (27) Stockman, M. In *Surface-Enhanced Raman Scattering: Physics and Applications-Topics in Applied Physics*; Kneipp, K., Moskovits, M., Kneipp, H., Eds.; Springer: Heidelberg, Germany, 2006; Vol. 103, pp 47–66.
 (28) Stockman, M. I.; Shalaev, V. M.; Moskovits, M.; Botet, R.; George, T. F. *Phys. Rev. B* **1992**, *46*, 2821–2830.
 (29) Haiss, W.; Thanh, N. T. K.; Aveyard, J.; Fernig, D. G. *Anal. Chem.* **2007**, *79*, 4215–4221.

RESULTS AND DISCUSSION

Figure 1 compares gold nanoparticles generated by laser ablation and in a chemical preparation process. Small spheres of relatively uniform sizes with a tendency to form aggregates or chains are obtained after ablating gold from the bulk material. The uniform size of the spheres can be between 7 and 30 nm depending on the applied laser intensity (images A in Figure 1a,c). Images B display gold nanoparticles prepared in a chemical reduction process. The extinction spectra of the ablation gold nanoparticles and their small aggregates or chains composed from spheres of relatively uniform sizes and the chemically prepared gold nanoparticles are very similar, with a plasmon resonance around 520 nm typical for gold nanospheres of sizes that are small compared to the wavelength of light (see traces A and B in Figure 1b). Obviously, the formation of small aggregates or chains composed from nanospheres of similar sizes does not strongly influence the extinction spectrum. Nanoaggregates consisting of spheres of different sizes (see image C in Figure 1a) are generated due to ablation *and* interaction of the laser with the suspended ablated gold spheres. Such aggregates of nanospheres with significantly different radii have been called nanolenses, since they can greatly enhance local optical fields by forming nanoscale hot spots in the gaps between the spheres.²⁶ As trace C in Figure 1b shows, nanoaggregates consisting of nanospheres of different sizes show in addition to the resonance around 520 nm, plasmon resonances over the entire near-infrared range also.

Figure 1c illustrates different geometries of nanolenses (type C). For comparison, it also shows small ablation aggregates composed from gold nanospheres of about the same sizes (type A). In the simplest case, the radii and spacing distances between the spheres of a nanolense form approximately a geometric series (see for example, structures shown in Figure 1c). This geometry is theoretically discussed in ref 26. Here, attempting to simulate clusters of the type present in the upper right corner of image C in Figure 1a, we consider a different geometry where the minimum radius nanosphere is sandwiched between two larger neighbors, as depicted in the schematic shown in Figure 2. The mechanism of the nanofocusing for this configuration remains the same as discussed in ref 26. Subjected to the optical electric field of the excitation wave, the larger nanosphere (the left one in the schematic of Figure 2a) forms in its vicinity a local optical field enhanced by a factor that is on the order of (in the exact surface-plasmon resonance) or less than (out of the resonance) the quality factor of the surface plasmon resonance, $Q \sim -\text{Re } \varepsilon / \text{Im } \varepsilon$, where ε is the dielectric permittivity of the metal at the surface-plasmon resonance frequency. For the case of gold in the near-infrared (NIR) region, it is $Q \sim 10$. This enhanced local field plays the role of the excitation field for the smaller nanospheres of this cluster. This next in size nanosphere responds in-kind and generates a field enhanced by a factor less than or on the order of $Q^2 \sim 100$. The fields at the minimum-size nanosphere in this case can be estimated as less than or on the order of $Q^3 \sim 10^3$. Because a plasmonic metal such as gold has a high absolute permittivity in the red spectral region, the potential drop at the surface of the metal is relatively small, and high local optical fields are generated in the gaps between the minimum-radius nanosphere and its neighbors. Quantitative computations were done similarly to ref 26 for gold nanolenses consisting of three

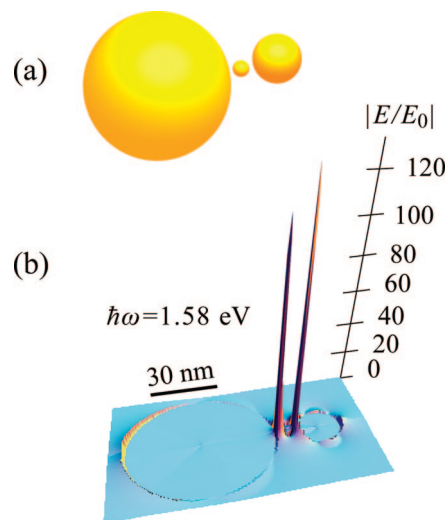


Figure 2. Nanolens geometry and distribution of local optical field. (a) Schematic of the nanolens geometry. Shown are three gold nanospheres with radii and small surface-to-surface gaps adapted from typical nanostructures such as shown in the right top corner of the electron micrograph of structure C in Figure 1. (b) Distribution of local field E relative to the excitation field E_0 in the symmetry plane of the nanolens. In agreement with the experimentally applied excitation wavelengths in the near-infrared, the photon energy of the excitation radiation is $\hbar\omega = 1.58$ eV, its polarization is along the axis of the nanolens. The local field enhancement $|E/E_0|$ is plotted along the vertical axis. Suggested nanoscale of sizes (30 nm) is indicated at the bottom.

nanospheres whose geometry is illustrated in Figure 2a, using permittivity data for gold.³⁰ The radii of the nanoparticles have been chosen to be 30:3.3:10 nm (from left to right in Figure 2a) to better conform with the requirements of the quasistatic approximation. The results of quantitative computations displayed in Figure 2b confirm the above-mentioned qualitative picture. The maximum local field E (the “hottest spot”) is predicted at the axis in the gap between the smallest and medium nanospheres where it is enhanced with respect to the excitation field E_0 by a factor $|E/E_0| \sim 130$. As well-known,²⁷ the SERS signal is proportional to $|E/E_0|^4$, which yields an enhancement factor of $\sim 3 \times 10^8$ for this hottest spot. This is in approximate agreement with ref 26. As theoretical calculations indicate (results not shown), the SERS enhancement only weakly depend on the exact ratio of the sizes of the constituent nanospheres in a nanolens as long as these sizes differ significantly and are within the range of the applicability of the quasistatic approximation (from nanometers to a few tens of nanometers). The physical reason for this property is that within the framework of the quasistatic approximation, the surface plasmon resonance frequency does not depend on the nanosphere size and neither does the local field enhancement. Thus, for such a nanolens of n nanospheres, the enhancement coefficient is estimated approximately as $\sim Q^n$, irrespectively of the specific sizes of the nanospheres. We checked this property numerically for the size ratio from 2 to 3 and found it to be valid within a few tens percent. For larger nanolenses, there are deviations from the quasistatic approximation due to the electrodynamic effects.³¹ These effects may lead either to further enhancement of SERS

(30) Johnson, P. B.; Christy, R. W. *Phys. Rev. B* **1972**, *6*, 4370–4379.

(31) Dai, J.; Cajko, F.; Tsukerman, I.; Stockman, M. I. *Phys. Rev. B* **2008**, *77*, 115419-1–115419-5.

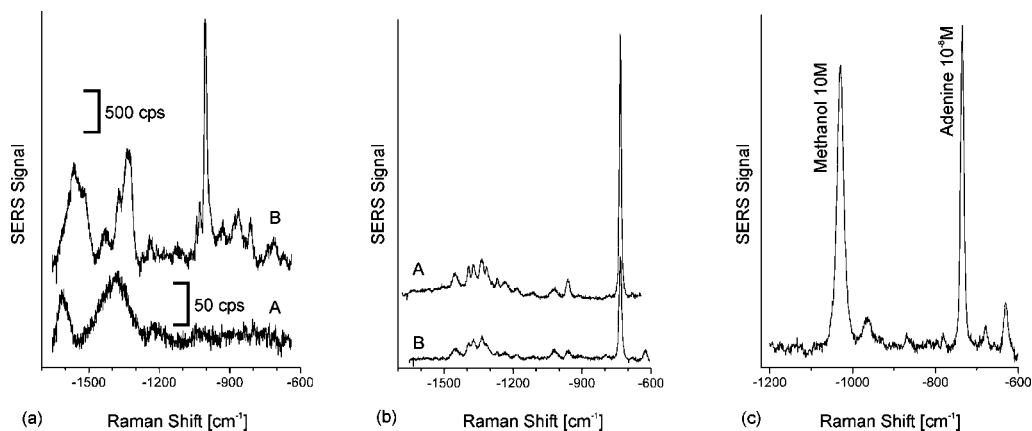


Figure 3. Comparison of SERS using gold nanolenses made by ablation and chemically prepared nanoaggregates as enhancing nanostructures. (a) Raman spectra measured from aqueous solutions of gold nanoaggregates without any analyte to compare background signals. The chemically prepared gold nanoparticles (spectrum B) display surface enhanced Raman lines, resulting from impurities introduced during the preparation process of this particular batch of colloids, such as the line at $\sim 1000\text{ cm}^{-1}$. The bands around 1500 cm^{-1} in the spectrum of the ablation nanoaggregates can be assigned to carbonate complexes.¹⁸ Spectra were measured at 50 mW at 785 nm excitation in 10 s (spectrum A) and 1 s (spectrum B) collection times. Abbreviation: cps, counts per second. (b) SERS signals of adenine measured in solutions of ablation aggregates (spectrum A) and chemically prepared nanoaggregates (spectrum B) using 10 mW at 785 nm excitation. (c) Comparison of the Raman signal of 10^{-8} M adenine and 10 M methanol measured in aqueous solutions of nanoaggregates.

due to electrodynamic resonances or to some suppression of it. In summary, the observed heterogeneity of the nanolens geometry (see for example structures C in Figure 1) is not expected to change principally the expected magnitude of SERS enhancement.

Gold nanolenses are also experimentally evaluated regarding their potential for SERS. As mentioned above, aside from the SERS enhancement factor, the Raman background level, generated by impurities on the surface of the enhancing nanostructures, is an important parameter in characterizing the capabilities of SERS-active substrates for ultrasensitive detection and identification of analytes. Figure 3a compares solutions of gold nanolenses made by ablation and gold nanoclusters prepared in a chemical reduction process regarding their Raman background signals. Nanolenses made by laser ablation show more than 10 times weaker background features with almost no bands in the wavenumber range below 1300 cm^{-1} . It should be noted that not all chemically prepared colloids exhibit such drastic impurities as shown in Figure 3a, in fact most do not, but that each batch of colloid needs careful testing prior to SERS experiments.

SERS enhancement factors of the ablation gold nanostructures were inferred from SERS measurements on adenine at 785 nm excitation. Since this molecule absorbs in the UV, the NIR excitation makes sure that no molecular resonance Raman process contributes to the observed enhancement.

Figure 3b compares SERS spectra of adenine measured in solutions of aggregates formed by significantly different-sized gold nanospheres (structures C in Figure 1) and chemically prepared gold nanoaggregates. Both structures provide enhancement at the same order of magnitude. The ring breathing mode of adenine at 735 cm^{-1} appears even at about three times higher signal level for the ablation structures than for the chemically prepared nanoclusters.

In contrast, experiments using ablation gold nanospheres and their aggregates formed by uniform-size spheres (structures A in Figure 1) did not give rise to a measurable SERS signal. This is a strong indication that the observed SERS enhancement on ablation aggregates formed by significantly different-sized gold

nanospheres results from the strong electromagnetic enhancement due to nanolenses.²⁶

The absolute SERS enhancement factor can be inferred from a comparison of the 735 cm^{-1} SERS signal of the 10^{-8} M adenine and the 1030 cm^{-1} line of methanol (not surface-enhanced), which was added to the sample solution in 10 M concentration. Taking into account the different concentrations of adenine and methanol, the same signal level of both Raman lines indicates a SERS enhancement factor on the order of 10^9 .

This SERS enhancement on the order of 10^9 represents a minimum enhancement, since it implies that all adenine molecules contribute to the SERS signal, which is not necessarily the case in most experiments. On the other hand, 10^{-8} M adenine molecules compared to 10^{-9} – 10^{-10} M gold nanoparticles arranged in the nanolenses and relatively wide gaps between the nanospheres could enable almost all molecules to find a place in the hottest spots in order to be involved in the SERS process at this level of enhancement. The experimentally observed enhancement factor of $\sim 10^9$ is also in approximate agreement with theoretical estimates for the hottest spots in these structures (cf. Figure 2). This reasonable agreement of theoretical and experimental enhancement factors appears due to relatively large gaps between individual particles. For $\sim 1\text{ nm}$ gaps adopted for our computations, the theoretical model may work reasonably well, whereas for smaller gaps we cannot, at this stage of the theoretical development, reliably solve the electrodynamic problem due to the effects on nonlocal dielectric response, electron spill-out, and others.³²

It should be noted that an enhancement factor on the order of 10^9 is still 4–5 orders of magnitude below experimentally observed enhancement factors for colloidal gold clusters formed from gold spheres during an aggregation process induced by added salt.³³ The relatively small enhancement factor obtained for the nanolenses can be understood in terms of their morphology depicted

(32) Pustovit, V. N.; Shahbazyan, T. V. *Chem. Phys. Lett.* **2006**, *420*, 469–473.

(33) Kneipp, K.; Kneipp, H.; Manoharan, R.; Hanlon, E. B.; Itzkan, I.; Dasari, R. R.; Feld, M. S. *Appl. Spectrosc.* **1998**, *52*, 1493–1497.

in parts a and c of Figure 1, structures C. Compared to “NaCl-induced” gold clusters, nanoaggregates made by laser ablation exhibit relatively large interparticle distances (gaps). The local concentration of fields and SERS enhancement strongly depend on the intersphere gaps and decrease when gaps increase.³⁴ By the way, these relatively wide gaps also explain the extremely poor SERS enhancement of ablation nanoaggregates built from uniform-size goldspheres (see for example structure type A in Figure 1c) compared to almost “touching” nanoparticles in chemically prepared gold aggregates (see Figure 1a, image B). The dramatic increase in enhancement factor in the case of ablation nanoaggregates comprised from gold spheres of different sizes appears to be due to the nanolens effect, despite the relatively large gaps.

Overall, 10^9 , as it has been achieved in the reported nanolenses, is a powerful enhancement factor for many analytical applications, and “wider gaps” of about 1 nm provide space for high numbers of analyte molecules to experience this enhancement level.

(34) Nordlander, P.; Oubre, C.; Prodan, E.; Li, K.; Stockman, M. I. *Nano Lett.* **2004**, *4*, 899–903.

(35) McCreery, R. L. *Proc. SPIE-Int. Soc. Opt. Eng.* **1992**, *25*, 1439.

(36) Baraga, J. J.; Feld, M. S.; Rava, R. P. *Appl. Spectrosc.* **1992**, *46*, 187–190.

(37) Frank, C. J.; Redd, D. C. B.; Gansler, T. S.; McCreery, R. L. *Anal. Chem.* **1994**, *66*, 319.

(38) Kneipp, J.; Kneipp, H.; Kneipp, K. *Proc. Natl. Acad. Sci. U.S.A.* **2006**, *103*, 17149–17153.

(39) Bidault, S.; de Abajo, F. J. G.; Polman, A. *J. Am. Chem. Soc.* **2008**, *130*, 2750–2751.

Moreover, gold nanolenses are very stable, as indicated by no measurable changes in the extinction spectra of their aqueous solution for more than 3 years. Broad plasmon resonances in the near-infrared (NIR) range allow free selection of the excitation wavelengths in a range, which is now very attractive for Raman spectroscopy,³⁵ particularly also for Raman studies of biological objects.^{36,37} Plasmon resonances in the NIR are also required for two-photon probing based on surface enhanced hyper-Raman scattering.³⁸ The chemically clean preparation not only prevents background SERS signals, it also opens up favorable conditions for a controlled modification and tailoring of the SERS active surfaces by a well-defined introduction of specific surface ions and molecules. The size of the nanolenses of ~100 nm or less along with plasmon resonances optimized for excitation in the NIR, as well as their chemically clean surfaces, which provide excellent conditions for functionalization, makes them potent structures for SERS nanosensors for targeted chemical probing in small biological structures, such as cells.

After finishing and submitting our manuscript, we found in the literature another way to design nanolenses, i.e., well-defined groupings of 5, 8, and 18 nm diameter Au particles with nanometer spacing using DNA templates.³⁹

Received for review January 30, 2008. Accepted April 13, 2008.

AC8002215